ELSEVIER

Journal of Chromatography A, 702 (1995) 97–112

JOURNAL OF CHROMATOGRAPHY A

Complete design of a simulated moving bed

Frédéric Charton, Roger-Marc Nicoud*

Séparex, B.P. 9, F-54250 Champigneulles, France

Abstract

The operating conditions of a simulated moving bed working under conditions of non-linear chromatography are difficult to find experimentally. A design procedure based on the modelling of multi-component chromatography is described. This rigorous and general procedure can be applied provided that basic data characterizing the experimental system are available. Even if the main parameters to be set are the flow-rates (one internal flow-rate and three out of four inlet/outlet flow-rates), it is explained how other free working parameters can be chosen. Special attention is paid to the column length, mobile phase velocity and particle size. It is shown how strongly they can influence the performance of a simulated moving bed.

1. Introduction

There is considerable interest in the preparative applications of liquid chromatography. In order to make the chromatographic process more attractive, attention is focused on the choice of the operating mode. Among the alternatives to the classical process (elution chromatography), much attention is currently being paid to the simulated moving bed (SMB) [1].

SMB technology was introduced in the late 1950s [2] and has mainly been applied to very large-scale production in the petrochemical and sugar industries [3]. However, separations of pharmaceutical compounds have recently been performed using an SMB [4,5] and other application areas are now opened up such as the fine chemistry, cosmetics and perfumes industries [6].

Different configurations of counter-current adsorption processes have been described [7]. However, the four-zone cascade of the Sorbex type [2] has been demonstrated to be the most efficient [8]. Fig. 1 shows a true moving bed (TMB) made of four zones; "true" refers to an actual circulation of solid and a zone is a coun-

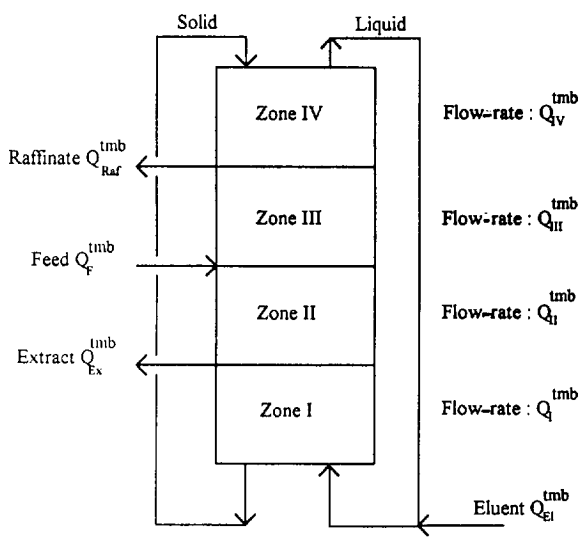

Fig. 1. Schematic representation of a four-zone TMB.

* Corresponding author.

0021-9673/95/$09.50
SSDI 0021-9673(94)01026-9

ter-current absorber where the fluid flow-rate is constant and, as explained below, is bordered by an injection point and a collection point. A TMB allows one to perform continuous chromatographic fractionations of binary mixtures (or pseudo-binary mixtures) into two streams of pure components (or pseudo-components). Two inlet lines allow one to inject continuously the solution to be separated (feed) and the eluent. Two outlet lines (extract, raffinate) allow one to withdraw continuously the pure products. The liquid flowing out of zone IV is recycled to zone I, whereas the solid coming out of zone I is recycled to zone IV.

In fact, it is extremely difficult to operate a TMB because it involves the circulation of a solid adsorbent [7], which is why a simulated moving bed [2] is suitable. Most of the benefit of a true counter-current operation can be achieved by using several fixed-bed columns in series and an appropriate shift of the injection and collection points [7]. Fig. 2 shows a schematic representation of an SMB: each zone is divided into identical subsections (in practice, a subsection is a fixed-bed column) and, in order to simulate a counter-current flow, the feed, eluent, extract and raffinate lines are all moved one column forward in the fluid flow direction at fixed time intervals (period). The greater the number of subsections (or columns) per zone the closer is an SMB to a TMB. In fact, an SMB with a small number of columns per zone (usually 2–4) shows almost the same performances as a TMB [7].

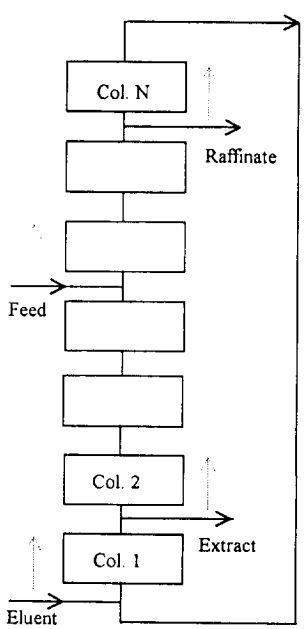

Fig. 2. Schematic representation of a four-zone SMB.

In this paper, we give the steps to be followed when designing an SMB which would allow one to process a given amount of feed per month. The procedure described is based on the modeling of non-linear chromatography, an experimental procedure being likely to fail unless the adsorption isotherms are linear (which is very uncommon in fact or means working at very low concentrations). It is a rigorous, versatile and general procedure. It mainly requires the determination of competitive adsorption isotherms, which is not so tedious and does not require as much work as is sometimes claimed. A few competitive adsorption data, measured using the mixture to be separated (the pure components are not necessary), are usually sufficient to find the operating conditions of an SMB [5].

The parameters we want to evaluate are the following: feed concentrations; number of columns per zone; column length, column diameter; particle size; and recycling (i.e., flow-rate occurring in zone I according to an arbitrary definition chosen in this paper) and inlet/outlet flow-rates. We assume that the following data are available, determined from a laboratory-scale study: equilibrium adsorption isotherms; relationship giving the height equivalent to a theoretical plate versus the mobile phase interstitial velocity u (Van Deemter equation); and relationship giving the pressure drop in the column (per unit length) $\Delta P/L$ versus the mobile phase velocity u (Kozeny–Carman equation).

2. Theory

2.1. TMB and SMB: two equivalent processes

The TMB and SMB concepts are similar. In fact, it has been shown that an SMB and hypothetical TMB whose operating conditions are

Table 1
Relationship between an SMB and its corresponding TMB

TMB	SMB
Steady state	Periodic steady state
Solid flow-rate	Periodic shift of the injection/collection lines
$\dot{M}$	$\Delta T = \frac{(1-\varepsilon)V_c}{\dot{M}}$
Internal flow-rates	Internal flow-rates
Q_k^{tmb} k = I, II, III or IV	$Q_k^{smb} = Q_k^{tmb} + \frac{\varepsilon}{1-\varepsilon} \cdot \dot{M}$
Eluent, extract, feed, raffinate flow-rates	Eluent, extract, feed, raffinate flow-rates
$Q_{EL}^{tmb}/Q_{Ex}^{tmb}/Q_F^{tmb}/Q_{Raf}^{tmb}$	$Q_{EL}^{smb}/Q_{Ex}^{smb}/Q_F^{smb}/Q_{Raf}^{smb}$

related through the rules in Table 1 [7] have very close performances [9]. Knowing that optimum operating conditions can be found directly for a TMB and that to simulate this kind of process leads to much shorter computation times, it is in our interest to take advantage of this similitude when designing an SMB. Consequently, the design of an SMB should as far as possible resort to the study of its corresponding hypothetical TMB.

The rules in Table 1 just mean that the velocity of the liquid relative to the solid is kept constant. V_c is the volume of one SMB column. The inlet/outlet flow-rates of an SMB and its corresponding TMB are identical. An SMB does not exactly work in a steady state but in a periodic steady state: during a given period, the internal concentration profiles vary, but the internal profiles examined at the same time for two successive periods are identical (except for a one-column translation).

It must be pointed out that a TMB internal concentration profile and consequently some of its performance (the extract and raffinate concentrations and the eluent consumption), depends on only four dimensionless internal flow-rates defined as $q_k^{tmb} = Q_k^{tmb}/\dot{M}$ (k = I, II, III or IV) and no longer on the solid flow-rate.

The average SMB and TMB internal flow-rates Q_m^{smb} and Q_m^{tmb} are related through

$$Q_m^{smb} = Q_m^{tmb} + \frac{\varepsilon}{1-\varepsilon} \cdot \dot{M} = \left(q_m^{tmb} + \frac{\varepsilon}{1-\varepsilon} \right) \dot{M} \quad (1)$$

where

$$Q_m^{tmb} = \frac{\sum_{k=1}^{4} Q_k^{tmb}}{4} = \frac{\dot{M} \sum_{k=1}^{4} q_k^{tmb}}{4} \quad (2)$$

The SMB average interstitial mobile phase velocity is defined relative to Q_m^{smb} as

$$Q_m^{smb} = \varepsilon u_m \Omega \quad (3)$$

where ε is the bed external porosity and Ω the column cross-section.

2.2. Adsorption isotherms

In the case of a single-component system, the adsorption isotherm gives the concentration in the stationary phase $\bar{C}$ versus the mobile phase concentration C when equilibrium is reached, at a given temperature. Even if it can sometimes be linear in a wide concentration range, the $\bar{C}$ vs. C relationship is usually not linear.

In the case of a multi-component mixture, there is usually a competition between the various compounds to access to the adsorption sites. Consequently, $\bar{C}_i$ does not only depend on C_i

but on all liquid-phase concentrations. Each component adsorption isotherm is a relationship of the type $\bar{C}_i = \bar{C}_i(C_1, C_2, \ldots)$.

Many different isotherm equations have been described [10]. Even though it has been challenged because it does not agree with the Gibbs' adsorption isotherm unless all saturation capacities are identical [11], the competitive Langmuir isotherm is often used:

$$\bar{C}_i = \frac{\bar{N}\tilde{K}_i C_i}{1 + \sum_j \tilde{K}_j C_j} \tag{4}$$

where $\bar{N}$ is the saturation capacity, assumed here to be equal for all components, and $\tilde{K}_i$ is a numerical coefficient quantifying the affinity of the solute towards the solid.

In fact, the Langmuir isotherm often fails to fit experimental data and more complex isotherms, such as the modified competitive Langmuir [4] or bi-Langmuir isotherm [12], are suitable. This is especially true with systems exhibiting concentration-dependent apparent selectivities $(\bar{C}_j/C_j)/(\bar{C}_i/C_i)$.

2.3. Equilibrium stage model

Many different models have been applied to the modelling of chromatographic processes [1]. The equilibrium stage model has been shown to be suitable under the usual conditions of high-performance preparative chromatography [13].

The column is considered as an association of cells in series. The adsorption equilibrium is assumed to be reached in each cell, called the equilibrium stage or plate. The broadening effects, linked to the mass transfer kinetics and to the hydrodynamics, are lumped together and are quantified by the number of theoretical plates N which can be derived from an "analytical" pulse injection.

In the case of fixed-bed operations (elution chromatography, SMB, etc.), the mass balance equation for a component i over a plate k is

$$C_{i,k-1} = C_{i,k} + \tau \cdot \frac{dC_{i,k}}{dt} + \tau \cdot \frac{1-\varepsilon}{\varepsilon} \cdot \frac{d\bar{C}_{i,k}}{dt} \tag{5}$$

where τ is the mean residence time of the mobile phase in a plate and ε the external porosity, which is usually in the range 0.35–0.45.

The equilibrium stage concept can also be applied to true moving bed adsorbers [14]. The mass balance equation of a component i over a plate k is

$$C_{i,k-1} + \frac{\dot{M}}{Q} \cdot \bar{C}_{i,k+1} = C_{i,k} + \frac{\dot{M}}{Q} \cdot \bar{C}_{i,k} + \tau \cdot \frac{dC_{i,k}}{dt} + \frac{(1-\varepsilon)}{\varepsilon} \cdot \tau \cdot \frac{d\bar{C}_{i,k}}{dt} \tag{6}$$

where Q and $\dot{M}$ are the fluid and solid flow-rates.

Various numerical methods are available to solve first-order differential equations such as Eqs. 5 and 6 when associated with a set of boundary and initial conditions [15]. We use the Gear's algorithm [16] implemented in the software LSODI belonging to the ODEPACK package [17], which is suitable here because it can handle "stiff" variations of the concentrations.

The steady state of a TMB can be calculated directly without solving Eqs. 6, which leads to much shorter computation times. Assuming the TMB steady state, Eqs. 6 can be simplified into Eqs. 7 when cancelling the accumulation terms:

$$QC_{i,k-1} + \dot{M}\bar{C}_{i,k+1} = QC_{i,k} + \dot{M}\bar{C}_{i,k} \tag{7}$$

where $\bar{C}_{i,k}$ and $C_{i,k}$ are related through the isotherm equations. Eqs. 7 are coupled non-linear algebraic equations and can be solved using a Newton–Raphson method [18].

2.4. Height equivalent to a theoretical plate

The height equivalent to a theoretical plate, H, is defined as

$$H = \frac{L}{N} \tag{8}$$

where L is the column length. It can be related to the experimental system parameters through the Van Deemter [19] or Knox [20] equations, which especially give H as a function of the interstitial mobile phase velocity u. In the case of preparative chromatography, where relatively

high velocities are used, these equations can often be simplified into a linear relationship [21–23]:

$$H = a + bu \tag{9}$$

The parameters a and b are related to the diffusion coefficient, porosity, mass transfer parameters, etc. If internal diffusion is the main resistance to mass transfer, their dependence on the particle diameter d_p is given by [24]:

$$a = Ad_p \tag{10}$$

$$b = Bd_p^2 \tag{11}$$

2.5. Pressure drop

The Kozeny–Carman equation is suitable for the laminar flows met with in chromatography:

$$\frac{\Delta P}{L} = h_k \cdot \frac{36}{d_p^2}\left(\frac{1-\varepsilon}{\varepsilon}\right)^2 \mu u = \frac{\varphi}{d_p^2} u = \Phi u \tag{12}$$

where h_k is the Kozeny coefficient (close to 4.5) and μ the eluent viscosity.

3. Results and discussion

The general procedure we use to design an SMB is described in Fig. 3. It mainly resorts to the equivalence between an SMB and its hypothetical corresponding TMB, as explained previously.

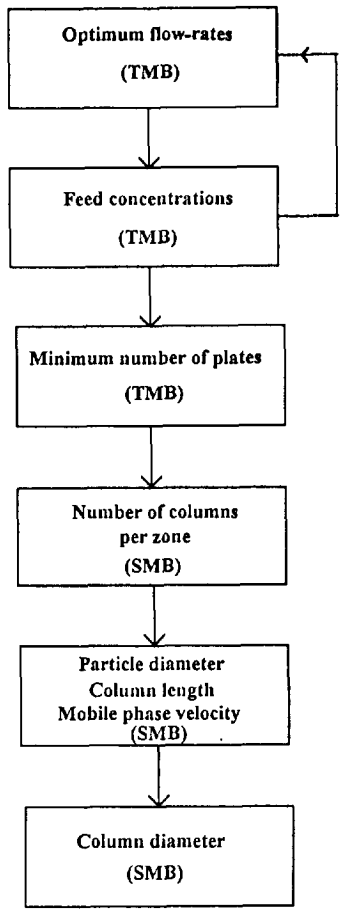

Fig. 3. Design of a simulated moving bed: procedure.

3.1. TMB optimum flow-rates

For a given feed composition, optimum flow-rates, i.e., giving the highest productivity and the lowest eluent composition, are estimated first for an "ideal system", which mainly means that kinetic and hydrodynamic dispersive effects are assumed to be negligible.

The conditions to be applied to TMB internal flow-rates have been broadly described [7]. In preparative chromatography, high feed concentrations are suitable and lead to non-linear adsorption behaviour. The non-linear (and related competitive) effects must be taken into account when evaluating the flow-rates. This issue has been barely addressed in the literature [25,26]. It is outside the scope of this paper to describe exactly the calculation procedure.

As an example, Fig. 4 gives the feed and eluent flow-rates versus the feed concentrations for the following competitive Langmuir isotherms: $\tilde{N} = 100$ g/l, $\tilde{K}_1 = 0.030$, $\tilde{K}_2 = 0.036$ ($\alpha = \tilde{K}_2/\tilde{K}_1 = 1.2$), when a total separation is sought. It shows how strongly the choice of the flow-rates is influenced by the feed concentrations.

At this point, for any given feed concentrations, the following flow-rates are available: q_k^{tmb}, q_F^{tmb}, q_{El}^{tmb}, q_{Ex}^{tmb}, q_{Raf}^{tmb}.

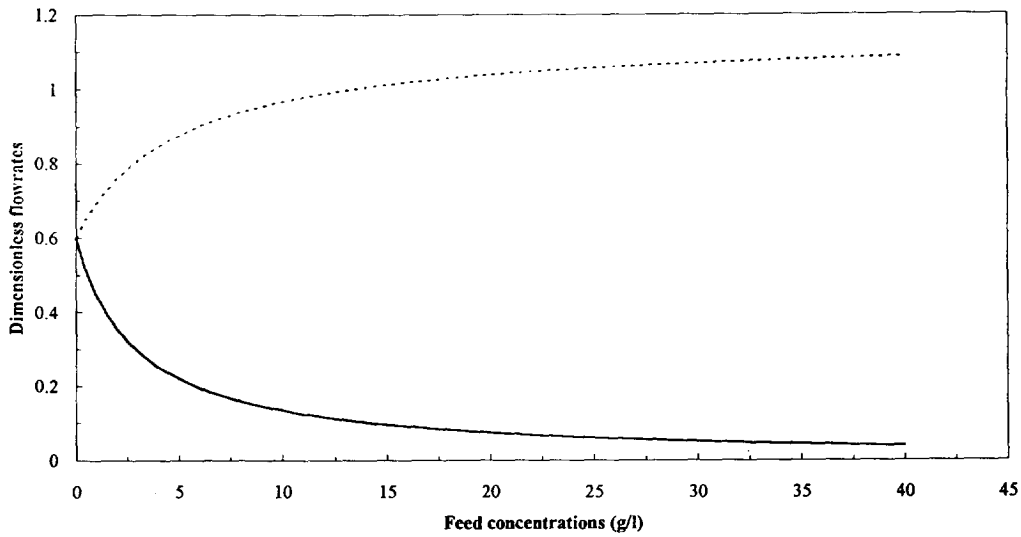

Fig. 4. Influence of the feed concentrations on an "ideal" TMB dimensionless feed (q_F^{tmb}) and eluent (q_{El}^{tmb}) flow-rates. Case of a 1:1 binary mixture with competitive Langmuir isotherms ($\tilde{N} = 100$ g/l, $\tilde{K}_1 = 0.030$ l/g, $\tilde{K}_2 = 0.036$ l/g). The continuous and dotted lines correspond to the feed and eluent flow-rates, respectively.

3.2. Feed concentrations

The feed concentrations have a strong influence on the SMB performances and must be well chosen. The productivity and the eluent composition are two main economic criteria involved in chromatographic processes [27]. Their variations versus the feed concentrations can be checked in order to choose an appropriate feed composition.

This study can be quickly carried out for an "ideal" TMB as mentioned in the previous section. For instance, Fig. 5 shows the variations of the productivity, written as $Q_F^{tmb} C_i^F$ assuming $\dot{M} = 1$ l/h, and of the eluent consumption in the case of the binary system of Fig. 4. The eluent

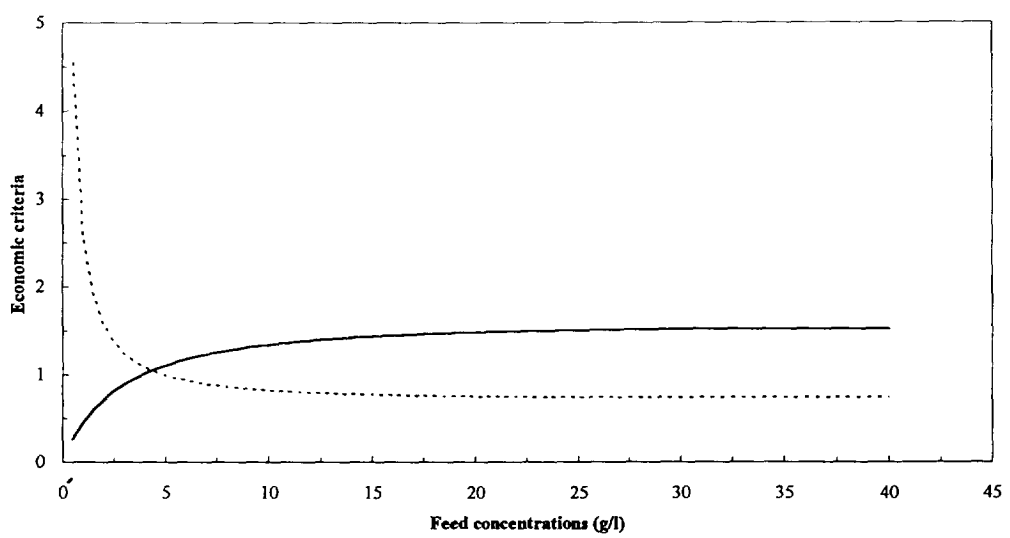

Fig. 5. Influence of the feed concentrations on an "ideal" TMB performance: dotted line, eluent consumption; continuous line, productivity for $\dot{M} = 1$ l/h. Experimental system as in Fig. 1.

consumption is the volume of eluent used to recover a unit mass of pure product and can be evaluated as $(Q_{El}^{tmb} + Q_{F}^{tmb})/Q_{F}^{tmb}C_i^F$. The productivity and eluent consumption have been derived from the flow-rates given in Fig. 4.

The productivity increases and the eluent consumption decreases when C_i^F increases; the variations are usually rather steep in the low concentration range and very smooth otherwise. As a consequence, low injection concentrations will have to be avoided. However, even if achievable, very high concentrations will not be suitable because as soon as concentrations are high enough the performances of the TMB (or SMB) are almost constant and very high concentrations can lead to a very low feed flow-rate, which might be difficult to control.

3.3. Number of plates requirement

The flow-rates given in Fig. 4 lead to 100% purities in the case of an "ideal" TMB. The approach used here is to keep these flow-rates and to seek the minimum number of plates N_m required to reach purities as high as 99%.

This procedure is sensible because it has been demonstrated that the performances of a TMB or SMB are only slightly sensitive to the number of plates [9]. In most instances, the number of plates required can easily be achieved and optimum flow-rates are then available.

The steady state of a TMB is calculated, as explained in the Theory section, for different numbers of theoretical plates, an identical number of plates in each zone being assumed. The extract and raffinate purities are derived from each numerical simulation.

Fig. 6 shows the evolution of the extract and raffinate purities versus the TMB total number of plates in the case of the system studied in Fig. 4 for a total feed concentration of 40 g/l; in the present instance, a TMB made of 400 plates (100 per zone) would give purities as high as 99%.

Fig. 7, which was constructed from numerical simulations, gives N_m as a function of the selectivity α and of the feed concentration, written as a dimensionless number $\tilde{K}_1 C_1^F$, in the case of competitive Langmuir isotherms and of a 1:1 binary mixture. Fig. 7 confirms that a very small number of plates is sufficient to obtain the purities expected, provided that conditions of linear chromatography do not prevail, i.e., when $\tilde{K}_1 C_1^F$ does not tend towards zero.

It must be understood that Fig. 7 can be used for all binary Langmuir isotherms provided that the saturation capacity is identical for the two

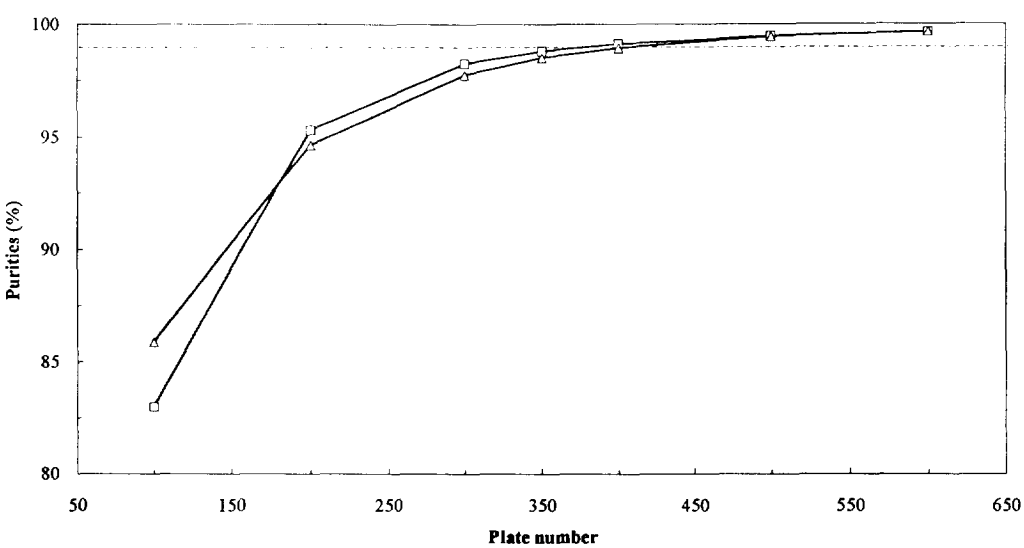

Fig. 6. Evolution of a TMB (□) extract and (△) raffinate purities as functions of the total number of plates. A TMB made of four identical zones (same number of plates per zone) is assumed. Case studied in Fig. 2 with $C_1^F = C_2^F = 20$ g/l.

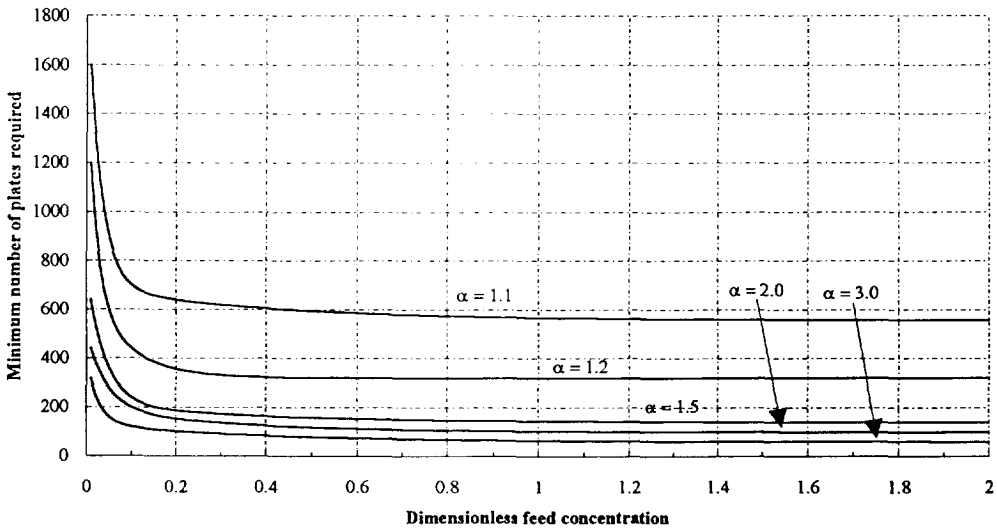

Fig. 7. Minimum number of plates required to reach purities higher than 99% as a function of the selectivity α and of the dimensionless feed concentration $\tilde{K}_1 C_1^F$. Case of 1:1 binary mixtures and competitive Langmuir isotherms with equal saturation capacities.

components. Actually, when introducing dimensionless concentrations $X_{i,k} = \tilde{K}_{i,k} C_{i,k}$ and $Y_{i,k} = \bar{C}_{i,k}/\bar{N}$ into Eqs. 6 in the steady state, it can be proved that N_m depends only on α, $\tilde{K}_1 C_1^F$ and the composition.

3.4. Number of columns per zone

The only way to estimate the number of columns per zone, N_c, is to perform numerical simulations of an SMB including the shift of the injection and collection points at regular time intervals. This kind of calculation can be performed using dummy values of the column volume and TMB solid flow-rate (to estimate the period ΔT). The SMB flow-rates are derived from the TMB flow-rates according to the rules summarized in Table 1.

For the system examined here, it was found out that an eight-column configuration (two columns per zone) was suitable. Fig. 8 compares the SMB (at the half-time period when the periodic steady state is reached) and TMB internal concentration profiles, confirming that the two processes have very close performances.

3.5. Column length and mobile phase velocity for a given particle size

We show here that there is an optimum choice of the column length L and of the average mobile phase velocity u_m which must fulfil plate number and pressure drop constraints.

In a previous section, a minimum number of plates requirement was derived in the case of a TMB made of four identical zones. In the case of an SMB, the internal flow-rate is different from one zone to another. Consequently, assuming identical columns, the number of plates for each column depends on its position (in zone I, II, III or IV). The plate number requirement should be applied to zone I where the internal flow-rate is the highest. However, in practice and for the sake of understanding, the plate number requirement can be applied relatively to the average number of plates per column (estimated with u_m). According to Eqs. 8 and 9, the plate number condition is fulfilled provided that

$$\frac{L}{a + bu_m} \geqslant \frac{N_m}{4N_c} \tag{13}$$

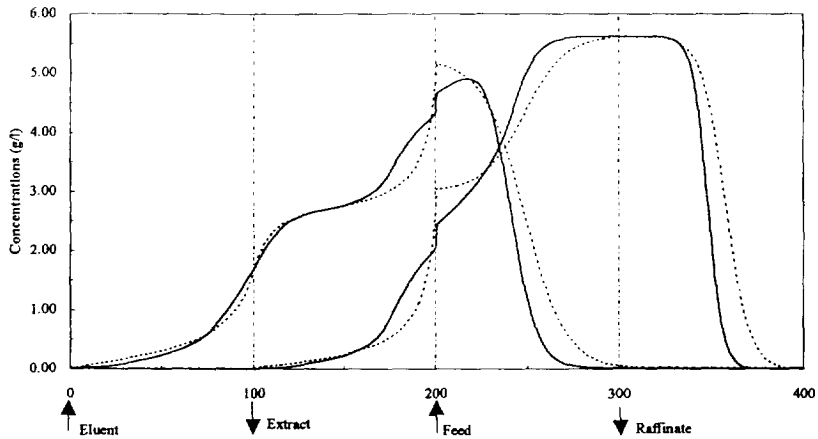

Fig. 8. Comparison between the internal concentration profiles of an SMB (at half-time period in steady state, continuous lines) and of its corresponding TMB (dotted lines). Case studied in Fig. 2 with $C_1^F = C_2^F = 20$ g/l. Total number of plates = 400, i.e., 100 plates per zone for the TMB and eight columns with 50 plates for the SMB.

which is equivalent to

$$\frac{L}{u_m} \geqslant \frac{N_m}{4N_c} \cdot \left(\frac{a}{u_m} + b\right) \tag{14}$$

The pressure drop condition leads to the following equation, which compares the pressure drop in the system (given according to Eq. 12) to the maximum pressure acceptable, P_{max}:

$$\frac{L}{u_m} \leqslant \frac{P_{max}}{4N_c} \cdot \frac{1}{\Phi u_m^2} \tag{15}$$

The hatched area of Fig. 9 gives all the

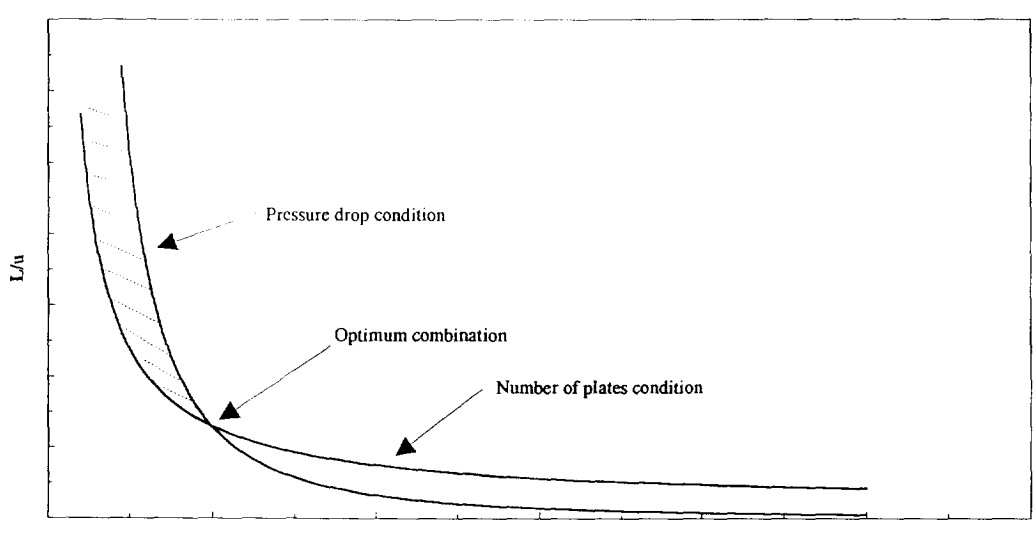

Fig. 9. Schematic representation of the possible values of the ratio L/u_m as a function of u_m. Definition of the optimum combination (L, u_m).

possible values of L/u_m fulfilling simultaneously Eqs. 14 and 15. Every point of this hatched area corresponds to a combination (L, u_m).

The choice of the optimum combination is related to the economic criteria. The eluent consumption can be written as

$$V_i = \frac{Q_{El}^{smb} + Q_F^{smb}}{Q_F^{smb} C_i^F} = \frac{Q_{El}^{tmb} + Q_F^{tmb}}{Q_F^{tmb} C_i^F} = \frac{q_{El}^{tmb} + q_F^{tmb}}{q_F^{tmb} C_i^F} \quad (16)$$

It depends only on the TMB dimensionless internal flow-rates, which themselves depend only on the adsorption isotherms and on the feed concentrations.

The productivity can be estimated from

$$Pr_i = \frac{Q_F^{smb} C_i^F}{4N_c \varepsilon V_c} \quad (17)$$

and can also be written as Eq. 18 on replacing $\dot{M}$ by u_m according to Eqs. 1 and 3 and keeping in mind that $Q_F^{smb} = Q_F^{tmb}$:

$$Pr_i = \frac{q_F^{tmb} \dot{M} C_i^F}{4N_c \varepsilon V_c} = \frac{q_F^{tmb} C_i^F}{4N_c \left(q_m^{tmb} + \frac{\varepsilon}{1-\varepsilon} \right)} \cdot \frac{1}{\frac{L}{u_m}} \quad (18)$$

where q_F^{tmb} and q_m^{tmb} depend only on the isotherms and on the feed concentrations.

Eq. 18 proves that the highest productivity is reached for the smallest value of L/u_m compatible with the pressure drop and plate number conditions. As shown in Fig. 9, the optimum value of L/u_m is met when the two inequalities corresponding to Eqs. 14 and 15 are just fulfilled.

The optimum average mobile phase velocity is the positive root of a quadratic equation and is given by

$$u_m = \frac{1}{2} \left[-\frac{a}{b} + \sqrt{\left(\frac{a}{b}\right)^2 + \frac{4P_{max}}{b\Phi N_m}} \right] \quad (19)$$

The optimum column length and ratio L/u_m can be derived from

$$L = \frac{1}{2} \cdot \frac{N_m}{4N_c} \left[a + b\sqrt{\left(\frac{a}{b}\right)^2 + \frac{4P_{max}}{b\Phi N_m}} \right] \quad (20)$$

$$\frac{L}{u_m} = \frac{N_m}{4N_c} \left[\frac{2a}{-\frac{a}{b} + \sqrt{\left(\frac{a}{b}\right)^2 + \frac{4P_{max}}{b\Phi N_m}}} + b \right] \quad (21)$$

Eq. 21 justifies the procedure followed here to design an SMB and especially the choice of the "minimum number of plates required". Actually, if the plate number is higher than N_m, L/u_m will be higher and the productivity lower. If the plate number is lower than N_m, the flow-rates of an "ideal" TMB no longer allow one to reach the purities expected. Other flow-rates have to be found. In any case, the feed flow-rate will be lower whereas the eluent flow-rate will be higher, leading to an increase in eluent consumption and possibly to a decrease in productivity.

The productivity refers here to the amount of purified product recovered per unit time and unit value of stationary phase immobilized. Another definition of the productivity has also been used in the literature [28]. It refers to the amount of purified product collected per unit time and per unit section column. It can easily be shown, following the same idea, that the two definitions of the productivity lead to the same optimum combination (L, u_m).

As examples, Table 2 shows various ways to reach the 400 plates required for the separation studied in this paper. The results are given for two different stationary phases: high efficiency means 2500 plates for an analytical column (25 cm × 0.46 cm I.D.) with an eluent flow-rate of 1 ml/min and a 10-μm particle size; low efficiency

Table 2
Optimum combination (L, u_m): influence of the stationary phase efficiency

Parameter	High-efficiency phase		Low-efficiency phase	
d_p (μm)	10	40	10	40
u_m (cm/s)	1.1	1.1	0.35	0.36
L (cm)	1.9	29.2	5.9	93.0
L/u_m (s)	1.7	25.8	16.7	258.3

H(cm) = $2d_p$ (cm) + 31 870 (or 318 700)$d_p^2 u$ (cm/s). ΔP (bar) = [3.65 · $10^{-6}/d_p^2$ (cm^2)] · L(cm) · u(cm/s), i.e., $h_k = 4.5$, $\varepsilon = 0.4$, $\mu = 10^{-3}$ Pa s, $P_{max} = 60$ bar.

means 250 plates for the same experimental conditions. In fact, high efficiency refers to stationary phases such as silica (bonded or not), whereas low efficiency refers to some solid phases used to separate enantiomers (microcrystalline cellulose triacetate). The parameters used in Eqs. 9 and 12 to generate these results are given in Table 2 and are typical experimental values.

As mentioned above, the SMB number of plates requirement is very often weak, and the optimum combination can sometimes lead to unrealistic column lengths, as shown in Table 2. This is especially true in the case of industrial-sized columns with large diameters; as an example, a minimum column length of 5–10 cm would be required for a 20 cm I.D.

3.6. Particle size

In this section, the choice of the particle size is studied. To justify our way of arguing, it is necessary to note that similar stationary phases with different particle sizes usually have the same properties (e.g., specific pore volume, specific interfacial area, ligand concentrations). The adsorption isotherms should be independent of the bead diameter [28].

Again, the economic criterion to be optimized is the productivity as written according to Eqs. 17 and 18, keeping in mind that for each bead diameter the optimum combination (L, u_m) is given by Eqs. 19–21.

Substituting a by Ad_p and b by Bd_p^2 in Eq. 21, it is possible to study the influence of the particle size on the optimum value of L/u_m:

$$\frac{L}{u_m} = \frac{N_m}{4N_c} \cdot \left[\frac{2Ad_p}{-\frac{A}{Bd_p} + \sqrt{\left(\frac{A}{Bd_p}\right)^2 + \frac{4P_{max}}{B\varphi N_m}}} + Bd_p^2 \right] \quad (22)$$

It can be proved that L/u_m tends toward a minimum value $\varphi(AN_m)^2/4N_cP_{max}$ when d_p tends towards zero, whereas it tends towards ∞ when d_p tends towards ∞. These are two mathematical limits and it must be kept in mind that Eq. 11 is certainly no longer valid when d_p is too small. Eq. 22 shows that there is interest in using particles that are as small as possible.

However, it has been mentioned previously that unrealistic column lengths can be reached when applying Eqs. 19–21 in the case of high-efficiency stationary phases. A minimum column length condition often has to be taken into account. The choice of an optimum particle size is related to this latter condition. The equation $L = L_{min}$, where L depends on d_p according to Eq. 20 and L_{min} is the minimum column length acceptable, has to be solved.

As examples, Table 3 gives the optimum values of the particle diameter for the high-efficiency stationary phase in Table 2 for different minimum lengths acceptable. It also compares the values of the ratio L/u_m found for other particle diameters. For a given column length, if the beads are too small, the mobile phase velocity is limited by the pressure drop. If the particles are too large, the velocity must be kept small because of the number of plates

Table 3
Choice of the optimum particle size according to the minimum column length acceptable

Parameter	L_{min} = 10 cm			L_{min} = 20 cm		
d_p (μm)	10	23 (optimum)	40	20	33 (optimum)	60
u_m (cm/s)	0.21	1.12	0.37	0.41	1.13	0.33
L/u_m (s)	48.8	8.9	26.6	48.8	17.7	59.2

condition. Table 3, which gives realistic figures, show how critical the choice of the particle diameter can be. Of course, all bead diameters are not commercially available and the choice should be made as close to the optimum as possible.

Endele et al. [22] studied the influence of the particle size of spherical silica on column efficiencies. They found $b = Bd_p^{1.5}$ instead of $b = Bd_p^2$ as assumed here. In fact, Eq. 11 is valid when internal diffusion is the main limitation to mass transfer. However, this difference does not alter the qualitative results found, even if it could change Eq. 22.

The conclusions of this section do not take into account the influence of the particle size on the price of the stationary phase. To do so, another definition of the productivity including this effect, i.e., amount of pure compound recovered per unit time and unit price of stationary phase immobilized, could be used and the same study could be undertaken.

3.7. Column diameter

Let us assume a column of 1 cm^2 section. The average mobile phase velocity u_m being set at its optimum value, the solid flow-rate is derived from Eqs. 1 and 3. The corresponding feed flow-rate is derived from the relationship $Q_F^{smb} = Q_F^{tmb} = q_F^{tmb}\dot{M}$.

The solid and feed flow-rates are proportional to the column section. Consequently, the minimum column section required to process m_F g of feed per hour is derived from

$$\Omega = \frac{m_F}{Q_F^{smb}(C_1^F + C_2^F)} \tag{23}$$

where Ω is in cm^2, Q_F^{smb} in l/h, C_i^F in g/l and Q_F^{smb} is the feed flow-rate injected in a column of 1 cm^2 section.

Finally, a new value of the solid flow-rate can be calculated and the SMB operating flow-rates can be deduced from the "equivalence" rules summarized in Table 1.

3.8. Experimental applications

The procedure described in this paper has been demonstrated to be effective for many different separations performed using an SMB [4,5]. In this section, we focus on the resolution of the EMD 53986 enantiomers (a synthesis chiral intermediate from Merck, Darmstadt, Germany [29]).

The separation is performed at 25°C on 20–45-μm Celluspher, a chiral stationary phase prepared from cellulose tri(*p*-methylbenzoate) according to a Ciba-Geigy patent [30], using pure methanol as the mobile phase. It is achieved on a Licosep 12–26, an SMB made of up to twelve Superformance columns (Merck) of 26 mm I.D. and manufactured by Separex (Champigneulles, France). The objective of the separation is to recover each of the enantiomer with a very high purity (close to 99%).

Determination of isotherms

Binary competitive adsorption data are measured using an analytical column (150 × 4.6 mm I.D.) at 25°C, according to the "adsorption–desorption" procedure [10]. The following parameters are found:

$$\bar{C}_1 = 3.96C_1 + \frac{7.07C_1}{1 + 0.140C_1 + 0.317C_2}$$

(less retained enantiomer) (24)

$$\bar{C}_2 = 3.96C_2 + \frac{15.96C_2}{1 + 0.140C_1 + 0.317C_2}$$

(more retained enantiomer) (25)

The agreement between the experimental and calculated values of the solid-phase concentrations is shown in Fig. 10.

Choice of feed concentrations

In the present case, the solubility of the racemic mixture is limited to 8 g/l. The feed concentrations $C_1^F = C_2^F = 3.75$ g/l are chosen.

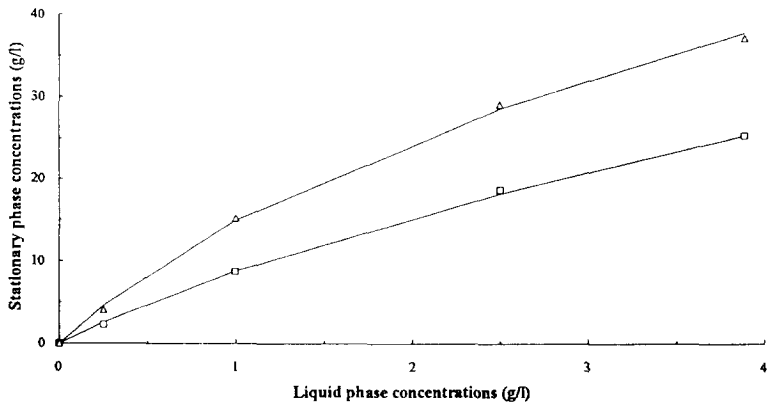

Fig. 10. Separation of EMD 53986 enantiomers. Comparison between experimental and calculated binary competitive adsorption data. Experimental data: △ = More retained enantiomer; □ = less retained enantiomer. Lines = data calculated.

TMB optimum flow-rates

Optimum dimensionless flow-rates are calculated for a hypothetical "ideal" TMB made of an infinite number of plates and a feed composition $C_1^F = C_2^F = 3.75$ g/l. The following operating flow-rates are found: $q_I^{tmb} = 19.92$, $q_{II}^{tmb} = 8.76$, $q_{III}^{tmb} = 11.16$, $q_{IV}^{tmb} = 8.66$. They can also be written as $q_I^{tmb} = 19.92$, $q_{Ex}^{tmb} = 11.16$, $q_F^{tmb} = 2.40$, $q_{Raf}^{tmb} = 2.50$.

Minimum number of plates required

Using the previous flow-rates, the steady state of a "real" TMB is calculated for increasing numbers of plates until the extract and raffinate purities are high enough. In the present case, 200 plates (50 per zone) lead to purities higher than 99%.

Number of columns per zone

An SMB with a total number of plates of 200 is assumed. The influence of the number of columns per zone is checked through numerical simulations (of an SMB) with dummy values of the column volume and solid flow-rate. The columns are assumed to be identical, equivalent to the same number of theoretical plates (i.e., $200/4N_c$ here). The flow-rates applied to the SMB are derived from the rules in Table 1 and using the "TMB optimum flow-rates". Table 4 gives the extract and raffinate purities calculated for various configurations of the process. As can be seen, an eight-column configuration is suitable. It must be pointed out that different numbers of columns could be implemented in each zone, but this possibility is not checked here.

Particle diameter, column length, mobile phase velocity

The particle size is not a free parameter. The optimum mobile phase velocity and column length, allowing one to reach 200 plates for eight columns in series and a maximum acceptable pressure of 40 bar, are sought. They are derived

Table 4
Influence of the number of columns per zone on the SMB performance

No. of columns per zone	Extract purity (%)	Raffinate purity (%)
1	96.4	99.2
2	99.6	99.8
3	99.7	99.9

from the following experimental equations and from Eqs. 19–22:

$$H\ (\text{cm}) = 1.35u\ (\text{cm/s}) + 0.01 \quad (26)$$

$$\Delta P = 2.41u\ (\text{cm/s}) \quad (27)$$

In the case studied, an average velocity u_m = 0.244 cm/s and an 8.5 cm column length are suitable.

The solid flow-rate is then estimated from Eqs. 1 and 3. With a porosity of 0.358, the solid flow-rate is $\dot{M}$ = 2.20 ml/min. The SMB operating conditions are calculated using Table 1: ΔT = 13.2 min, Q_I^{smb} = 44.9 ml/min, Q_{Ex}^{smb} = 24.4 ml/min, Q_F^{smb} = 5.4 ml/min, Q_{Raf}^{smb} = 5.5 ml/min.

Fig. 11 compares the SMB internal profiles, measured experimentally and calculated at the half-time period when the periodic steady state is reached. Fairly good agreement is obtained; the purities are slightly lower than expected (close to 97%). The purities can be increased, however, by slight adjustment of the flow-rates around the values evaluated first through the procedure described in this paper.

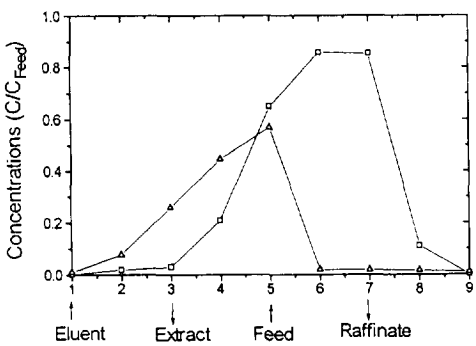

A

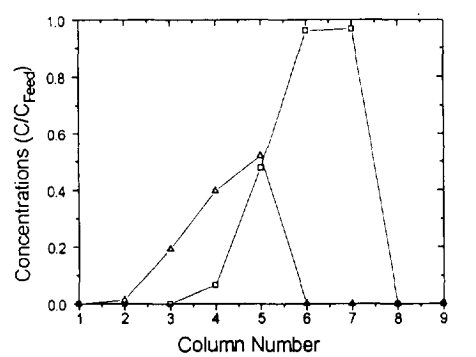

B

Fig. 11. Separation of EMD 53986 enantiomers. Comparison between the SMB (A) experimental (obtained on a Licosep 12–26) and (B) calculated internal concentration profiles. △ = More retained enantiomer; □ = less retained enantiomer.

4. Conclusions

A procedure allowing the design of an SMB has been described and the different steps to be followed have been briefly explained. The procedure can be used provided that data that can be determined according to classical experimental methods characterizing the system studied are available. It is general and can be applied to almost any kind of isotherm. It is a fast design procedure because it is not based on numerical empiricism, i.e. on a numerical "trial and error" method, but on an a priori guess of the flow-rates.

It has been shown that not only do the flow-rates have to be chosen carefully, but also other parameters such as the column length, the mobile phase velocity and the particle size. For a given bead diameter, the optimum column length and mobile phase velocity have been derived. Because an SMB does not require a high number of theoretical plates to work efficiently, the small particles used in classical preparative HPLC (i.e., in the 10–20-μm range) can lead to an unrealistic optimum column length. In this case, it has been proved that larger particles should be used. In fact, there is an optimum particle size related to the minimum column length condition.

The procedure described here is not only theoretical, it has been applied (at least partly) routinely to pilot-scale separations (i.e., with 2.5 cm I.D. columns) for a few years and we have begun to use it experimentally for industrial-scale separations (i.e., with 20 cm I.D. columns).

Symbols

a, b, A, B	coefficients relating the height equivalent to a theoretical plate to the mobile phase velocity (cm, s^{-1}, dimensionless, $cm^{-2}s^{-1}$, respectively)
C, C_i	mobile phase concentrations (g/l)
C, C_i	solid-phase concentrations (g/l)
$C_{i,k}, \bar{C}_{i,k}$	Concentrations of component i in plate k (g/l)
C_i^F	feed concentrations (g/l)
d_p	particle diameter (cm)
h_k	Kozeny coefficient
H	height equivalent to a theoretical plate (cm)
$\tilde{K}_i, \bar{N}$	isotherm parameters (1/g and g/l, respectively)
L	column length (cm)
L_{min}	minimum column length acceptable (min)
$\dot{M}$	solid flow-rate (ml/min)
m_F	amount of feed processed per unit time (g/h)
N_c	number of columns per zone
N	number of theoretical plates
N_m	minimum number of plates required
P_{max}	maximum pressure acceptable (bar)
Q	fluid flow-rate (ml/min)
Q_k^{tmb}, Q_k^{smb}	TMB and SMB internal flow-rates in zone k (ml/min)
Q_F	feed flow-rate (ml/min)
Q_{Ex}	extract flow-rate (ml/min)
Q_{Raf}	raffinate flow-rate (ml/min)
Q_{El}	internal flow-rate in zone k (ml/min)
$q_k^{tmb}, q_F^{tmb}, \ldots$	dimensionless TMB flow-rates
t	time (min)
u	interstitial mobile phase velocity (cm/s)
u_m	SMB average mobile phase velocity (cm/s)
V_c	SMB column volume (ml)
X, Y	dimensionless concentrations
ΔP	pressure drop (bar)
ΔT	period (min)

Greek letters

α	selectivity
φ, Φ	parameter relating the pressure drop to the mobile phase velocity (Pa s and Pa s/cm^2, respectively)
ε	external porosity
μ	mobile phase viscosity (Pa s)
τ	mobile phase residence time in a cell (min)
Ω	column cross-section (cm^2)

References

[1] G. Ganetsos and P.E. Barker (Editors), *Preparative and Production Scale Chromatography*, Marcel Dekker, New York, 1993.

[2] D.B. Broughton, *US Pat.*, 2 985 589 (1961).

[3] R.M. Nicoud, *LC·GC Int.*, 5 (1992) 43.

[4] R.M. Nicoud, G. Fuchs, P. Adam, M. Bailly, E. Küsters, F.D. Antia, R. Reuille and E. Schmid, *Chirality*, 5 (1993) 267.

[5] R.M. Nicoud, M. Bailly, J.N. Kinkel, R. Devant, T. Hampe and E. Küsters, in R.M. Nicoud (Editor), *Simulated Moving Bed: Basics and Applications*, INPL, Nancy, 1993, pp. 65–88.

[6] G. Hotier, in *Proceedings of the 9th Symposium on Preparative and Industrial Chromatography "Prep 92"*, INPL, Nancy, 1992, pp. 235–240.

[7] D.M. Ruthven and C.B. Ching, *Chem. Eng. Sci.*, 44 (1989) 1011.

[8] C.B. Ching, K.H. Chu, K. Hidajat and M.S. Uddin, *AIChEJ.*, 38 (1992) 1744.

[9] D. Tondeur and M. Bailly, in R.M. Nicoud (Editor), *Simulated Moving Bed: Basics and Applications*, INPL, Nancy, 1993, pp. 95–117.

[10] R.M. Nicoud and A. Seidel-Morgenstern, in R.M. Nicoud (Editor), *Simulated Moving Bed: Basics and Applications*, INPL, Nancy, 1993, pp. 4–34.

[11] M.D. Levan and T. Vermeulen, *J. Phys. Chem.*, 85 (1981) 3247.

[12] S. Jacobson, S. Golshan-Shirazi and G. Guiochon, *J. Am. Chem. Soc.*, 112 (1990) 6492.

[13] S. Golshan-Shirazi and G. Guiochon, *J. Chromatogr. A*, 658 (1994) 149.

[14] U.P. Ernst and J.T. Hsu, *Ind. Eng. Chem. Res.*, 28 (1989) 1211.

[15] B.A. Finlayson, *Non-Linear Analysis in Chemical Engineering*, McGraw-Hill, New York, 1980.

[16] W.H. Press, B.P. Flannery, S.A. Teukolsky and W.T. Vetterling, *Numerical Recipes in Pascal*, Cambridge University Press, New York, 1989, Ch. 15.

[17] A. Hindmarsh, in R.S. Stepleman, M. Carver, R. Psekin, W.F. Ames and R. Vichnevetsky (Editors), *Scientific Computing*, North-Holland, Amsterdam, 1983.
[18] W.H. Press, B.P. Flannery, S.A. Teukolsky and W.T. Vetterlin, *Numerical Recipes in Pascal*, Cambridge University Press, New York, 1989, Ch. 9.
[19] J.J. Van Deemter, F.J. Zuiderweg and A. Klinkenberg, *Chem. Eng. Sci.*, 5 (1956) 271.
[20] J.H. Knox, *J. Chromatogr. Sci.*, 15 (1977) 352.
[21] Cs. Horváth and H.J. Lin, *J. Chromatogr.*, 149 (1978) 43.
[22] R. Endele, I. Halasz and K. Unger, *J. Chromatogr.*, 99 (1974) 377.
[23] D.M. Ruthven and C.B. Ching, in G. Ganetsos and P.E. Barker (Editors), *Preparative and Production Scale Chromatography*, Marcel Dekker, New York, 1993.
[24] J. Villermaux, in A.E. Rodrigues and D. Tondeur (Editors), *Percolation Processes: Theory and Applications*, Sijthoff & Noordhoff, Alphen aan de Rijn, 1981.
[25] H. Rhee, R. Aris and N.R. Amundson, *Philos. Trans. R. Soc. London*, 269 (1971) 187.
[26] C.B. Ching, C. Ho and D.M. Ruthven, *Chem. Eng. Sci.*, 43 (1988) 703.
[27] R.M. Nicoud and M. Bailly, in *Proceedings of the 9th Symposium on Preparative and Industrial Chromatography "Prep 92"*, INPL, Nancy, 1992, pp. 205–220.
[28] A. Felinger and G. Guiochon, *J. Chromatogr.*, 591 (1992) 31.
[29] K. Brandt and J. Nagel, *Eur. Pat.*, 0 450 504 (1990).
[30] E. Francotte and G. Baisch, *Eur. Pat.*, 0 136 270 (1988).